EVALUATION OF DUMMY SHOULDER KINEMATICS IN OBLIQUE FRONTAL COLLISIONS

Fredrik V. Törnvall, Kristian Holmqvist, Johan Davidsson and Mats Y. Svensson
Department of Applied Mechanics, Chalmers University of Technology,
Göteborg, Sweden

Jörgen Gugler and Hermann Steffan
Vehicle Safety Institute, Graz University of Technology
Graz, Austria

Yngve Håland
Autoliv Research, Vårgårda, Sweden

ABSTRACT

The present study evaluates shoulder kinematics of the Hybrid III and THOR NT, with the first version of a new shoulder design (SD-1), in 45° far-side, full frontal and 30° near-side collisions. In total eleven dummy tests were conducted in the three collision angles, while film and instrument data were generated and compared with those of PMHS data from Törnvall (2008). For the 45° far-side impact, the THOR SD-1_{NT} dummy retained the shoulder belt on the shoulder during on-loading, as did the PMHSs, whereas the THOR NT did not. In the 30° near-side impact, the superior motion of the belted THOR SD-1_{NT} shoulder resembled that of the PMHSs.

Keywords: Shoulder, Kinematics, PMHS, Sled tests

A significant number of severe and fatal injuries occur in offset and oblique frontal collisions. Regulatory and consumer tests have encouraged designs of vehicles with increased safety in the crash situations they represent, however crashes which correspond to load paths similar to those of the EuroNCAP and the USNCAP crash test protocols accounted for only 23% of the belted fatalities in frontal collisions in Sweden (Lindquist et al. 2004). On the other hand small overlap crashes, defined as smaller than 30% overlap and with the drive train excluded as an active load path, account for 48% of the belted fatalities in frontal collisions in Sweden (Lindquist et al. 2004). Furthermore, Buzeman (1997) concluded that the MAIS 2+ and MAIS 3+ injury risks in near-side 2/3 offset collisions were significantly higher than in full-frontal or far-side offset collisions. Buzeman also showed that the MAIS 3+ injury risk was higher for the far-side 2/3 and 1/3 offset collisions than for the full-frontal ones. Hontschik and Rüter (1980) found that an occupant moving away from the shoulder belt anchor can result in the torso slipping out of the shoulder belt. Lindquist et al. (2006) analyzed small-overlap crashes, from which they concluded that the torso of the occupants was forced in a rotational oblique, anterior-lateral direction towards the side structure of the vehicle.

The results generated in these studies emphasize the importance of conducting crash tests in offset and oblique collisions to further reduce traffic related injuries. Such crash tests require access to crash test dummies that replicate the human body motion in oblique impacts. It is likely that, in these oblique collisions, the shoulder will influence important parameters such as head kinematics, head contacts with restraints or the car interior, and chest loads.

The Hybrid III 50th percentile male is currently the dummy most widely used in crash tests, regardless of whether the tests are full-frontal, offset or oblique. Its head kinematics in frontal flexion is unfortunately not adequately human-like (Thunnissen et al. 1995; Wismans and Spenny, 1984). Moreover, the Hybrid III may be stiffer in the lumbar spine than the human, especially in oblique crashes (Lindquist et al. 2006). Its shoulder complex lacks a clavicle-like structure, which is critical to the shoulder belt interaction, and is an essentially stiff structure with a range-of-motion smaller by a factor of three than the human shoulder complex (Törnvall et al. 2005b).

The THOR is a more advanced successor to the Hybrid III, with improved biofidelity (White et al. 1996; Hoofman et al. 1998; and Shaw et al. 2000). The first THOR dummy version was made available in 1999, the THOR Alpha in 2001 (Haffner et al. 2001) and the New Technology (THOR NT) in 2005. The most recent version has the dynamic responses of the Alpha, while offering enhanced durability and ease of use (Onda et al. 2006). Meanwhile, the European frontal impact dummy project developed the THOR FID Technology dummy (THOR FT), which improved the THOR Alpha dummy. Compared with the Hybrid III, the THOR dummy has, among other things, improved rib-cage geometry and shoulder design with an integrated clavicle structure that can move in the anterior and posterior directions.

Several studies have investigated THOR head and thorax kinematics in full-frontal impacts (Shaw et al. 2000; Vezin et al. 2001 and 2002; Kent et al. 2003; and Shaw et al. 2005). Few studies have compared the human shoulder response with that of the frontal impact dummies of today; Vezin et al. (2002) compared the shoulder response of a Hybrid III and a THOR Alpha with that of PMHSs in a full-frontal test set-up. In static conditions, the THOR shoulder range-of-motion was assessed and found to be smaller, by a factor of three, than that of the human shoulder (Törnvall et al. 2005b). In another study of THOR, it was indicated that its shoulder may not be adequately biofidelic in oblique far-side tests, which caused the occupant to move inboard in the vehicle and to slip out of the shoulder belt more easily than did the PMHSs (Törnvall et al. 2005a). A new shoulder for the THOR NT, designated THOR SD-1_{NT}, with more human-like shoulder geometry and range-of-motion, was therefore developed by Törnvall et al. (2007).

This study aims to evaluate the shoulder kinematics of the Hybrid III, THOR NT and THOR SD-1_{NT} in 45° far-side collisions (here, far-side is inboard occupant motion, away from the shoulder belt anchor), as well as in 30° near-side collisions (here, near-side is outboard occupant motion, towards the shoulder belt anchor) with that of PMHSs tested by Törnvall (2008). Full-frontal collisions were conducted as a reference.

METHODS

In parallel with the PMHS experiments carried out by Törnvall (2008), a Hybrid III, THOR NT and THOR SD-1_{NT} (Figure 1) were tested in frontal and angled impacts. The THOR SD-1_{NT} is in brief a THOR NT with new shoulders design (SD). The SD has been presented by Törnvall et al. (2007) and evaluated in static test conditions using volunteers Törnvall et al. (2005b). In brief, the SD comprises a humanlike clavicle bone with humanlike curvature and joint locations, and a scapula replica that incorporates the bone landmarks of the human counterpart and a linkage system that allow for motion relative the spine box in anterior, superior and lateral directions.

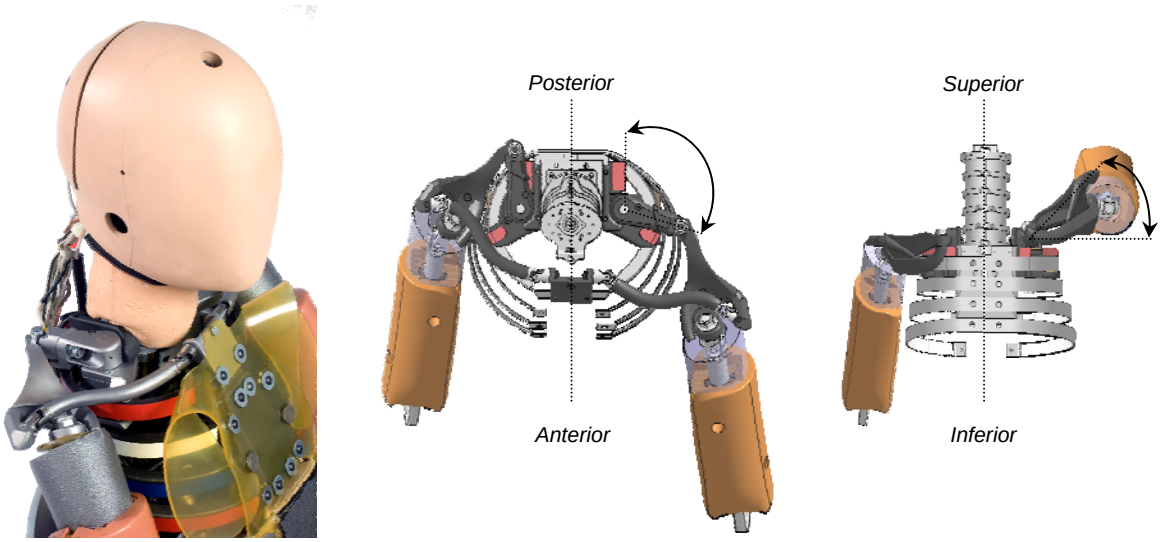

Fig. 1 – Schematic of the THOR SD-1_{NT}, oblique photo of the structure representing the clavicle and shoulder (left) and schematics of the possible SD-1 motions.

EXPERIMENTAL DESIGN:
In brief, the PMHSs and dummies were instrumented, fitted with film targets, positioned in a rigid laboratory seat mounted on an acceleration sled, and exposed to full-frontal, far-side, and near-side collisions. The subjects were restrained by means of a three-point belt, an upper anchorage point to the right, and a simplified car door interior which was installed to the right of the test subject (Figure 2).

Test Subjects: Dummy anthropometry was in the range of those of the PMHSs (Table 1). In the PMHS tests, the subjects were made to be seated in erect spine posture by means of some devices. Consequently, to simulate the posture of the PMHSs, the THOR dummies' spine posture was adjusted to be erect prior to testing. All dummies were positioned in the seat with the H-point corresponding to the R-16 standards (UN, 1958b), hands placed in their laps, their backs made to rest against the seat back and their necks adjusted in a vertical position. After each test, the dummies were examined for damage.

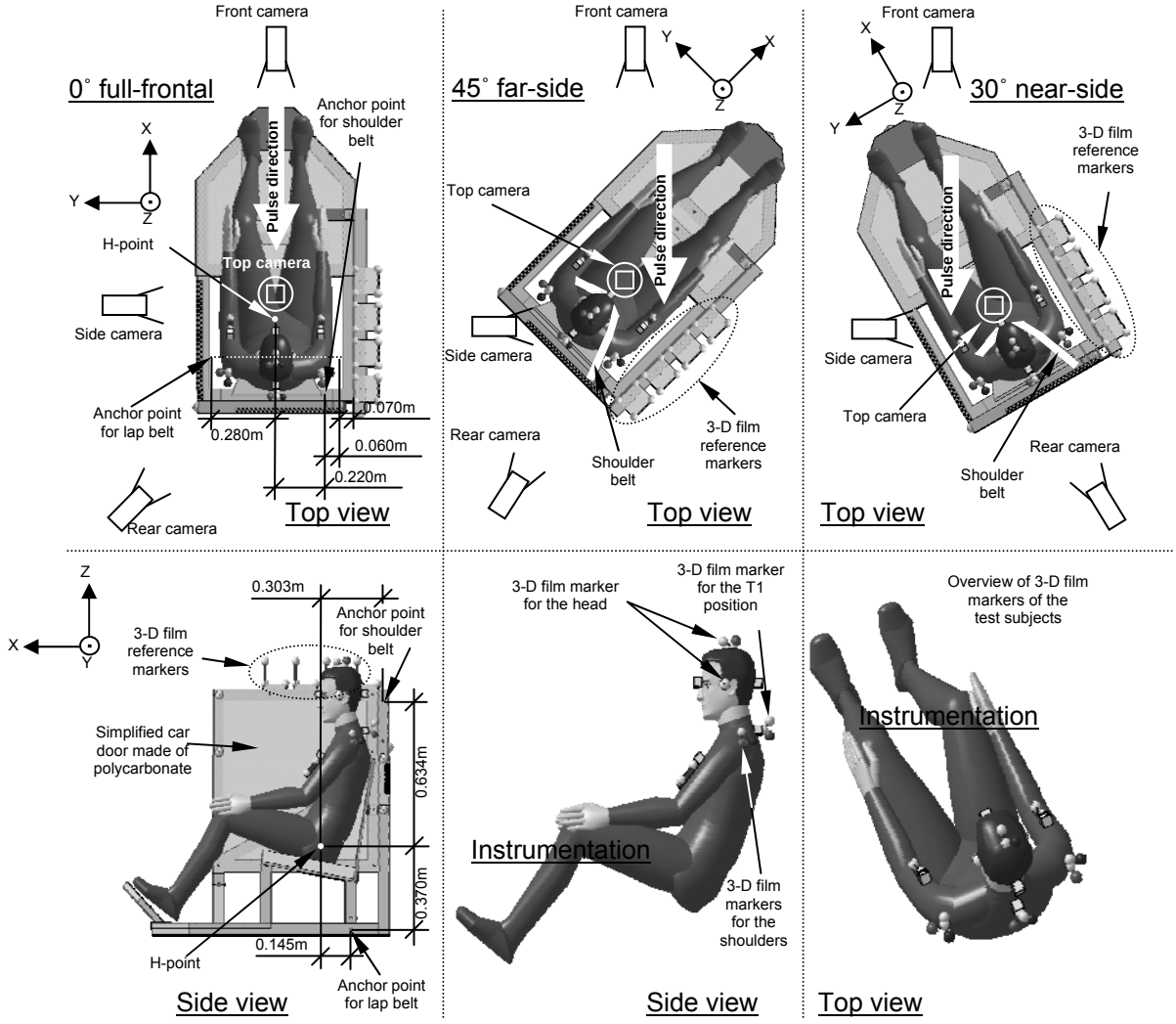

Fig. 2 – Top: Test set-up of the three included test conditions. Bottom: Instrumentation of the test subjects.

Instrumentation: All dummies were with fitted film targets which were screwed to the metal structure at the top of the skull, the superior-posterior part of the spine box, the shoulder structures and upper arms. The spine box and shoulder film targets were positioned to resemble those of the average PMHS T1 and shoulder targets, which were mounted to the acromion, respectively.

Table 1. PMHSs and dummy anthropometry data.

Parameter [year/kg/m]	PMHS 1	PMHS 2	PMHS 3	Hybrid III	THOR NT	THOR SD-1_{NT}
Sex	F	M	M	M	M	M
Age	84	59	71	–	–	–
Weight	62	61	94	78	77	76
Height	1.64	1.66	1.79	–	–	–
Occipital-chin circum.	0.68	0.63	0.71	0.67	0.67	0.67
Neck circum.	0.40	0.37	0.50	0.27	0.38	0.38
Upper arm circum.	0.33	0.27	0.30	0.31	0.31	0.31
Chest circum.	1.03	0.87	1.15	1.00	0.92	0.92
Chest depth	0.21	0.21	0.30	0.27	0.24	0.24
Chest width	0.33	0.30	0.39	0.32	0.29	0.29
Abdomen circum.	0.87	0.78	1.08	0.89	0.92	0.92
Upper body height (seat surface to acromion)	0.52	0.56	0.60	0.54	0.57	0.60
Sitting height	0.81	0.84	0.89	0.88	0.89	0.89
Biacromial shoulder width	0.35	0.37	0.41	0.35	0.35	0.40
Length of left clavicle	0.16	0.16	0.18	–	0.13	0.18
Length of right clavicle	0.16	0.15	0.18	–	0.13	0.18

Sled, seat and belt system: A pneumatic system made the sled accelerate (Figure 3 and Table 2). Average peak acceleration for all tests was 13.9 g and Δv was 26.6 km/h.

A R-16 seat (UN, 1958b), on which 50 mm deformable foam was placed between subject and seat cushion, was used in the study. The foam was made of polyethylene 220-E, 35 kg/m^3 and had a stiffness of 40 kPa at 10% compression, 55 kPa at 25% compression and 110 kPa at 50% compression. A 45° angled foot plate positioned according to R-16 was used to support the feet. A manual non-retractor belt with a continuous loop, three-point high-stretch webbing (16% stretch at 11.3 kN, Autoliv) without and force limiter were used. Belt attachment points were chosen as a compromise between the visibility of the film targets and commonly used attachment positions in production vehicles. The attachment points also complied with the R-14 regulation (UN, 1958a). In each test, a new belt was used. Belt position relative the shoulder was carefully reproduced in all tests. No steering wheel or air bag was used.

Table 2. Oblique frontal collision test conditions. All data CFC60 filtered.

Type of test	Subject	Test number	Δv [km/h]	Maximum sled acc. [g]
0° full-frontal	PMHS 1	16	27.0	13.3
	PMHS 2	19	27.1	13.6
	PMHS 3	22	24.9	12.6
	PMHS 3	23	25.6	12.5
	Hybrid III	13	27.2	14.1
	THOR NT	12	27.2	14.6
	THOR SD-1_{NT}	6	26.9	14.1
	THOR SD-1_{NT}	8	27.2	15.1
	THOR SD-1_{NT}	9	27.5	14.5
Averages for the 0° full-frontal tests			**26.7**	**13.8**
45° far-side	PMHS 1	17	27.0	13.7
	PMHS 2	20	27.5	14.4
	PMHS 3	24	25.5	13.2
	Hybrid III	14	25.9	14.2
	THOR NT	4	26.4	14.2
	THOR SD-1_{NT}	5	26.6	14.3
Averages for the 45° far-side tests			**26.5**	**14.0**
30° near-side	PMHS 1	18	27.1	13.5
	PMHS 2	21	27.0	13.6
	PMHS 3	25	25.7	12.9
	Hybrid III	15	26.4	14.2
	THOR NT	11	26.1	14.7
	THOR SD-1_{NT}	10	26.2	14.7
Averages for the 30° near-side tests			**26.4**	**13.9**

The simplified car door was made of a 10 mm thick sheet of polycarbonate, mounted vertically and parallel to the median plane of the seat. The distance from the sagittal plane to the door was 0.350 m (Figure 2) and resembles that of a medium to large car.

Data Acquisition and Analysis: Four MotionXtra HG-LE cameras recoded the events at 1000 f/s: front, side, rear and top view (Figure 2). The top and side view cameras were equipped with fixed 14 mm focal length lenses, while the front and rear cameras had fixed 20 mm focal length lenses. The film was analyzed, including tracking, scaling, and distance compensation, with TEMA Automotive™ Software. The head film marker data was recalculated to represent that of the head CG. All film data was filtered using CFC 20.

Coordinate System: All displacement data were produced according to the seat-fixed coordinate system or relative the T1 in the seat coordinate system (Figure 2) and taken as zero at impact start.

RESULTS

The data analysis focuses on an overview of the shoulder motions of the Hybrid III, THOR NT and THOR SD-1_{NT}, in comparison with PMHS data in three test configurations: 45° far-side, 30° near-side and 0° full-frontal collisions. Detailed 3-D kinematics can be found in Appendix A (X-Y trajectories) and B (displacements in relation to T1).

45° FAR-SIDE: In short, the head and T1 of the PMHSs and the dummies moved forward and laterally relative the seat during the initial phase of the 45° far-side tests (Appendix A). During the forward motion, the shoulder belt slipped along the clavicle or equivalent dummy structure from the sternal to the acromial end, for all PMHSs and the dummies. The heads of the PMHSs and dummies rotated and translated initially forward relative to T1 (Appendix A, 1).

Maximum anterior head CG displacement was reached between 157 and 167 ms for the PMHSs, 147 ms for the Hybrid III and 179 ms for the THOR SD-1_{NT}. The THOR NT data for the 45° far-side test was excluded after 140 ms because the shoulder belt slipped off the shoulder. Thereafter the belt was caught by the arm mounted accelerometer. The loaded shoulder displacement relative to T1 for all PMHSs and dummies includes a posterior and superior motion, except for PMHS 3 which initially moved inferior, and the THOR SD-1_{NT} which initially moved anterior (Appendix B, 4 and 6). All PMHSs and the THOR SD-1_{NT} displayed anterior and superior displacement of the non-loaded shoulder relative to T1. This was in contrast to the Hybrid III and THOR NT which did not move superior (Appendix B, 7 and 9).

The point defined as the time when the belt slipped off the shoulder was when the belt had slipped over an approximate line drawn from the coracoid process and passing through the humerus joint. This was determined by visual inspection of the high speed videos. A complementary identification of the escape time was carried out by analyzing the shoulder belt force. The time at which the test subjects slipped out of the seat belt was divided into two categories: “on-loading slip” was defined as the event when the subject slipped out before the maximum anterior head CG displacement, in relation to the sled, had occurred; “off-loading slip” took place when the subject slipped out after the maximum anterior head CG displacement, in relation to the sled, i.e. during the head rebound phase. None of the PMHSs or the Hybrid III and THOR SD-1_{NT} exhibited on-loading slip (Table 3). However, the THOR NT exhibited on-loading slip.

Table 3. Belt slippage during the 45° far-side tests

Belt geometry	Test subject	Belt slippage	Type of slippage
45° far-side	PMHS 1, Test 17	No slippage	–
	PMHS 2, Test 20	No slippage	–
	PMHS 3, Test 24	Belt slippage	Off-loading slip after approx. 170 ms
	Hybrid III, Test 14	Belt slippage	Off-loading slip after approx. 160 ms
	THOR NT, Test 04	Belt slippage	On-loading slip after approx. 130 ms
	THOR SD-1_{NT}, Test 05	No slippage	–

30° NEAR-SIDE: In the near-side collisions, the T1 and head of the PMHSs and dummies moved forward, in the reverse direction to that of the sled acceleration (Appendix A). During this motion, the shoulder belt slipped along the PMHS clavicle and the jacket surfaces of the dummies towards the necks. The belt then made its way into the soft tissue or dummy structure in the inferior region of the neck. Thereafter the heads rotated forward as the subjects started to load the shoulder belt (Appendix A, 1–2). The PMHSs reached their maximum anterior head CG displacement from 129 to 137 ms, the Hybrid III and THOR NT at 147 ms and the THOR SD-1_{NT} at 164 ms.

During the crash some contacts between subject and simplified car door interior occurred. The loaded shoulder and arm of PMHS 3 made contact with the simulated door at 115 ms, in contrast to those of PMHSs 1 and 2, which shoulders did not make contact with the door. All the dummy shoulders made contact with the car door: the Hybrid III at 125 ms, the THOR NT at 115 ms and the THOR SD-1_{NT} at 119 ms. The head of PMHS 1 made contact with the right arm which, in turn, made contact with the car door at 140 ms. The Hybrid III head did not make contact with the car door. For the others, the film targets mounted at the top of the heads make contact with the car door; PMHS 2 and 3 at 160 ms and 155 ms, respectively, THOR NT at 146 ms and, THOR SD-1_{NT} at 155 ms.

In relation to T1, the loaded shoulder moved anterior for PMHS 1 but posterior for PMHSs 2 and 3, whereas anterior for all dummies (Appendix B, 13). The loaded shoulder of the Hybrid III and the THOR NT moved slightly inferior to T1, whereas the loaded shoulder of the THOR SD-1_{NT} and all PMHSs moved superior to T1 during the loading phase (Appendix B, 15). For the non-loaded shoulder, the Hybrid III shoulder moved posterior relative to T1. This was in contrast to the shoulders of the THOR NT, the THOR SD-1_{NT} and the PMHSs, all of which moved anterior to T1 (Appendix B, 16). Moreover, the non-loaded shoulder moved superior to T1, initially, and then inferior to T1 for all dummies and PMHSs (Appendix B, 18).

0° FULL-FRONTAL: During the full-frontal collisions, the T1 and head CG markers of all subjects moved forward relative the seat (Appendix A). The shoulder belts restrained the loaded shoulders. As a consequence, the torsos rotated around a vertical axis. This rotation occurred for all PMHSs and dummies except for the Hybrid III.

The PMHSs reached their maximum anterior head CG displacement at 145-152 ms, the Hybrid III at 151 ms, THOR NT at 155 ms, and THOR SD-1_{NT} between 171–179 ms (3 tests). The loaded shoulder of all three PMHSs, the Hybrid III, and the THOR NT moved posterior to T1, while the THOR SD-1_{NT} moved anterior to T1 (Appendix B, 22). The non-loaded shoulder moved anterior to T1 for all PMHSs, the THOR NT and SD-1_{NT}. The anterior motion of the non-loaded shoulder was larger for the THOR SD-1_{NT} and smaller for the Hybrid III than that of the PMHSs. The loaded shoulders of PMHSs 1 and 2 moved superior to T1, in contrast to that of PMHS 3 (Appendix B, 24). Although the vertical motion of the loaded shoulder of the dummies fluctuated around zero, the THOR SD-1_{NT} fluctuated more than the Hybrid III and THOR NT. The non-loaded shoulders of PMHSs 1 and 2 moved inferior to T1, in contrast to the left shoulder of PMHS 3 (Appendix B, 27). However, the non-loaded shoulder of the Hybrid III and THOR NT fluctuated around zero, while the non-loaded shoulder of THOR SD-1_{NT} moved mostly inferior to T1.

DISCUSSION

This study aims to evaluate shoulder kinematics of the Hybrid III, THOR NT and THOR SD-1_{NT} dummies, in 45° far-side and in 30° near-side collisions, with that of PMHSs. Full-frontal collisions were carried out as a reference.

45° FAR-SIDE: In the 45° far-side tests, none of the PMHSs slipped out of the shoulder belt before maximum anterior head CG displacement occurred (Table 3): PMHSs 1 and 2 did not slip out of the shoulder belt at all, while PMHS 3 slipped out at 170 ms, during off-loading. The THOR SD-1_{NT} did not slip out of the shoulder belt; the Hybrid III showed off-loading slip at 160 ms. The THOR NT, however, showed on-loading slip at 130 ms (Table 3). High speed video data revealed that the Hybrid III torso did not rotate around its T1 Z axis in the full-frontal test. This lack of torso rotation, in comparison with the PMHSs, most likely contributed to the Hybrid III not slipping out of the shoulder belt. Thus, the Hybrid III belt interaction is not a consequence of a biofidelic shoulder complex, but rather a result of a stiff lumbar spine. Both Lindquist et al. (2006) and Törnvall et al. (2005a) also

found that the Hybrid III dummy has a somewhat stiffer lumbar spine than a human, especially in oblique crashes. Törnvall (2008) found indications that the shoulder belt of the PMHSs may have been caught by the coracoid process, thereby hindering the belt from slipping off the shoulder. Accordingly, the shoulder geometry of the THOR NT may explain why it showed on-loading slip in contrast to the PMHSs and the THOR SD-1_{NT}. Thus, it is reasonable to infer that the clavicle and coracoid process geometry of the THOR SD-1_{NT} shoulder hindered the belt from slipping off the shoulder in the 45° far-side collision.

30° NEAR-SIDE: In the 30° near-side impact the shoulder belt slipped along the clavicle or equivalent dummy structure towards the neck for all the PMHSs and the dummies. This off-loaded the lateral part of the shoulder. The anterior and superior motion of the arm, caused by its inertia, may then have caused the superior motion of the loaded shoulders of the PMHSs (Appendix B, 15). The medial and superior shoulder motion during loading may influence risk and time of contact with other objects, e.g. the car interior. These shoulder contacts could in turn affect the head kinematics and the risk and time of head-to-vehicle interior impacts in near-side impacts. Hence, the shoulder properties would also be of importance in frontal crash test dummies used in near-side collision testing. The loaded shoulder of the Hybrid III and the THOR NT did not allow for superior motion, which explains why these dummies did not replicate the superior motion of the PMHSs loaded shoulders (Appendix B, 15). However, the superior loaded shoulder motion of the PMHSs was replicated by the THOR SD-1_{NT}. As a consequence, the head CG of the THOR SD-1_{NT} dummy moved slightly more laterally (2 cm), towards the simulated car door than did the head CG of the THOR NT (Figure 4).

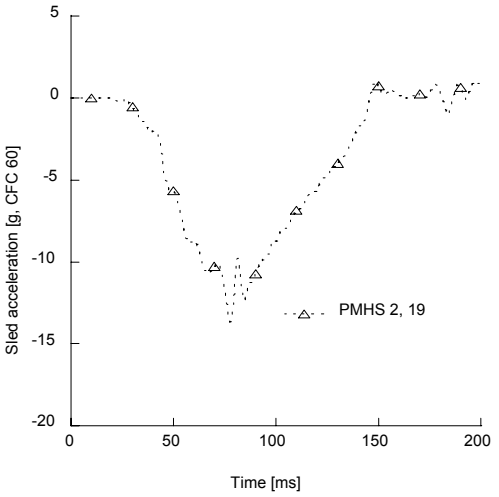

Fig. 3 – Sled pulse example (CFC 60, SAE J211, test number 19.

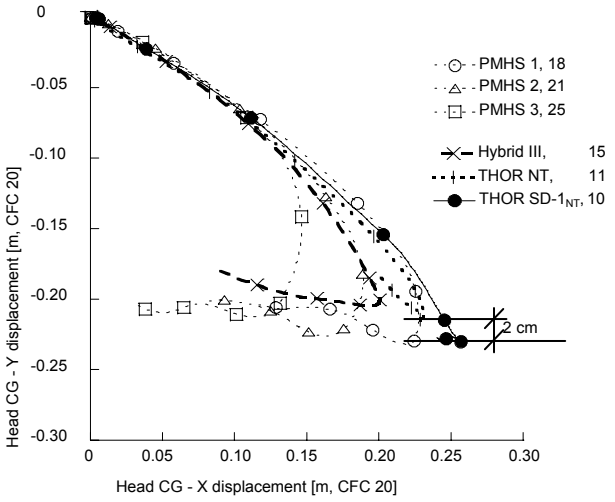

Fig. 4 – Head X-Y trajectories from the PMHSs and dummy tests in the 30° near-side test set-up

IMPACT VELOCITY: The average peak acceleration was 13.9 g and the average Δv was 26.6 km/h for both the dummies and PMHSs in this study. The relatively low pulse and Δv were a concession to limitations of laboratory space and capacity of the pneumatic accelerator. The advantage of the moderate impact severity was that the PMHSs did not sustain any detectable injuries; they could be used in several consecutive tests.

SHOULDER RANGE-OF-MOTION OF THE THOR SD-1_{NT}: In the 0° full-frontal collisions, the anterior non-loaded shoulder displacements in relation to T1 for the PMHSs were about 7 to 12 cm. However, for the THOR SD-1_{NT} the same shoulder displacement was about 21 cm (Figure 5). The THOR SD-1_{NT} shoulder range-of-motion was based on static relaxed volunteer shoulder test data. There are two complimentary explanations of why this dummy anterior range-of-motion, in particular, is larger than those of the PMHSs.

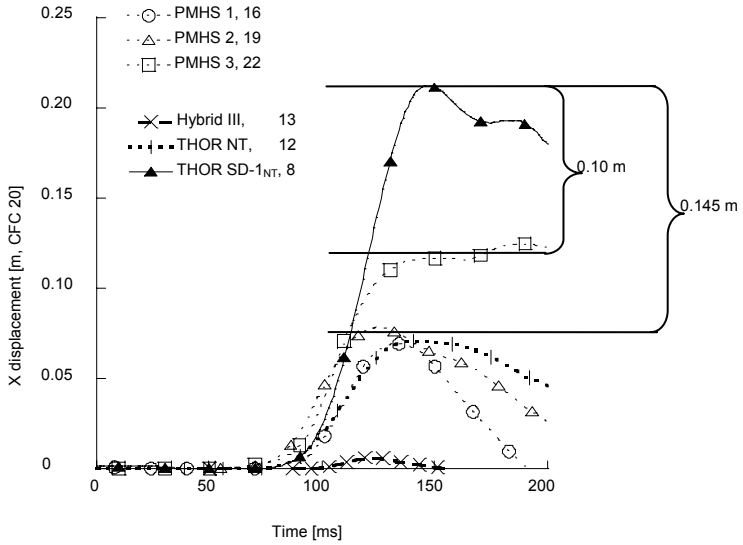

Fig. 5 – Non-loaded (left) anterior shoulder rel. to T1 displacements; PMHSs and dummies in full-frontal tests. One test per PMHS and one THOR SD-1_{NT} test are included.

First: Some additional range-of-motion was incorporated in the SD-1 design to account for larger range-of-motion during dynamic loading compared to static. Törnvall et al. (2007) performed static shoulder range-of-motion tests, in relation to the sternum of the THOR SD-1_{NT}, and compared the data with that of volunteers (Törnvall et al. 2005b). It is reasonable to believe that the volunteers did not have much remaining shoulder range-of-motion when loaded with the largest load (force, about 200 N/arm), since the displacement data indicated progressive stiffening for loads 150–200 N (Figure 6). To conclude, about 4 cm of the difference in the anterior shoulder motion of the THOR SD-1_{NT} can therefore be attributed to the fact that the SD-1 was designed with a larger anterior shoulder range-of-motion than that of the volunteers.

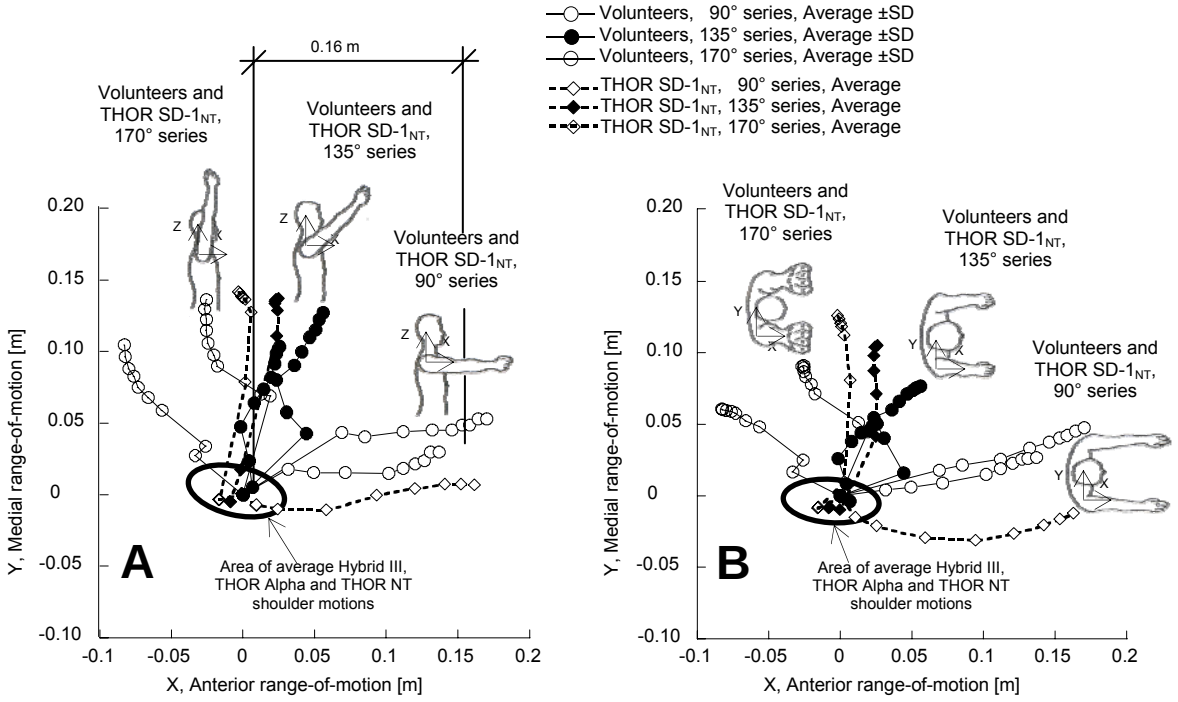

Fig. 6 – A and B: Averages of shoulder motions of the volunteers (average ±SD) and dummies in three static range-of-motion test series. A: Right side view. B: Top view. For each curve, the origin represents the neutral position, second point when the subject was connected to the load application cable, subsequent points represent an increase of 25 N/point/arm.

Second: The static volunteer shoulder range-of-motion tests conducted by Törnvall et al. (2005b) served as design values for the SD-1. In that study the sternum was used as the reference for the shoulder displacements, whereas in the present study the T1 was the reference; it was noted that the method used in the volunteer study generated excessive values. The reason for this was that the upper torso rotation inflated the values. Hence, a re-analysis of the volunteer tests (in which displacement relative to T1 was estimated) revealed that the anterior shoulder range-of-motion for the male volunteers was about 13 cm. Thus, about 3 cm of the difference in the anterior shoulder motion of the THOR SD-1_{NT} can be attributed to the SD-1 being designed with shoulder range-of-motion data referenced relative to the sternum instead of the T1.

These two explanations may account for about 7 cm of the 10 cm difference for left anterior shoulder motion in relation to T1, between PMHS 3 and THOR SD-1_{NT} (Figure 5). We have chosen to make this comparison only with PMHS 3 because of the similarities in biacromial shoulder width, clavicle length and upper body height for PMHS 3 and the THOR SD-1_{NT}. Furthermore, the evaluation was made only for the 0° full-frontal test (since that configuration has the fewest complex 3-D motions), which facilitates this reasoning and understanding of the shoulder motion. Moreover, the left shoulder was not influenced by belt to shoulder contact, which allowed for an unrestrained full range of shoulder motion. However, the range-of-motion is just one part of the shoulder properties. Very high priority should be given to the interaction with the shoulder belt. The resemblance to the human shoulder geometry, especially the clavicle and coracoid process, may also be critical; the SD-1 is an improvement in this respect.

HEAD AND T1 DISPLACMENETS MAY DEPEND ON MUSCLE TENSING: In the current study, the head, T1 and shoulder kinematics for dummies were compared with those of PMHSs. In the experiments and analysis, no compensation for possible pre-crash muscle tension was incorporated. The effect on time for peak excursion and kinetic response of such bracing is unknown.

RANGE-OF-MOTION MAY DEPEND ON OCCUPANT POSITION: In the present re-analysis of the static volunteer shoulder range-of-motion data, Törnvall et al. (2005b), we noticed that the shoulder moved 3.8 cm anterior to T1, when the arm positions were shifted from an unsupported position to when the first load of 25 N/arm was applied; the latter is similar to the driver having his hands on a steering wheel (Figure 7). This means that a driver has used up about 4 cm of the anterior range-of-motion when placing the hands on the steering wheel. This could also indicate that the anterior shoulder range-of-motion of the SD-1 should have been designed to be about 9 cm (13–3.8 cm) for a driver holding both hands on the steering wheel. Nevertheless, the discussion and reasoning above indicate that the anterior shoulder range-of-motion of the SD-1 must be reduced. Moreover, the dynamic anterior shoulder range-of-motion of the THOR NT (about 7 cm) may be close to that of humans (about 9 cm) in relation to T1, for a driver who holds both hands on the steering wheel, although this would be somewhat too small for a passenger with the hands in the lap (about 13 cm). As a consequence, the THOR NT shoulder response is more human-like than that of the Hybrid III. This finding is consistent with Vezin et al. (2002), who concluded that the THOR Alpha dummy had a more human-like response of the shoulder complex than the Hybrid III.

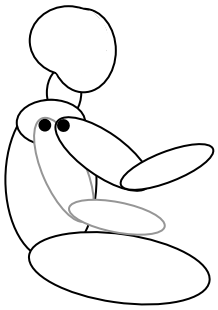

Fig. 7 – Schematic illustration of the shoulder location; hands in the lap and hands on steering wheel.

SIZES OF THE PMHS TEST SUBJECTS: The sizes of the PMHSs did not fully match a 50th percentile male. Differences in size could be compensated for by using scaling methods. Kerrigan et al. (2005) developed a scaling technique for pedestrian kinematics in a single plane. Unfortunately, this technique may not predict complex 3-D rotations and the belt-to shoulder interaction; e.g. it is not certain that the joint rotation of a small adult differs from that of an average adult. It may also be difficult to scale the sliding of the belt over the torso in an oblique impact situation. We are not yet aware of any scaling technique that takes into consideration complex 3-D rotations and an understanding of the belt-to shoulder interaction.

Mertz (1984) scaled the time-force response of the thorax by representing the system as a mass-spring one. However, Mertz scaling was developed and applied by dropping PMHSs to a surface and studying the lateral response of the thorax. In the present study the situation is more complex, since the body is loaded by a belt which may slide over the torso. The stiffness is not the same throughout the torso and may depend greatly on the load distribution (Kent et al. 2004 and Kent et al. 2005). In our oblique collisions the belt tended to slide over the torso and the shoulder. Hence, the shoulder belt loaded different regions of the thorax during the course of a collision. This means the stiffness may vary over time during an oblique impact because the shoulder belt slides over the torso and shoulder, which makes it difficult to estimate how the stiffness of the test subject changes. Body mass variation may also play a role which could be difficult to estimate. The head and arms may be viewed as free flying objects until the neck and arms are fully aligned in the direction of the acceleration pulse. Therefore we chose not to scale the 3-D kinematic data in this study.

REPEATABILITY OF THE SD-1: Repeated tests with a THOR SD-1_{NT} indicated that the SD-1 performance was repeatable in 0° full-frontal tests in the lateral direction, but it was less so in the anterior and inferior directions (Figure 8, A). The lack of repeatability may be caused by small variations in belt-to-shoulder interaction. However, the non-loaded SD-1 shoulder performed quite repeatably in all directions in the 0° full-frontal tests (Figure 8, B).

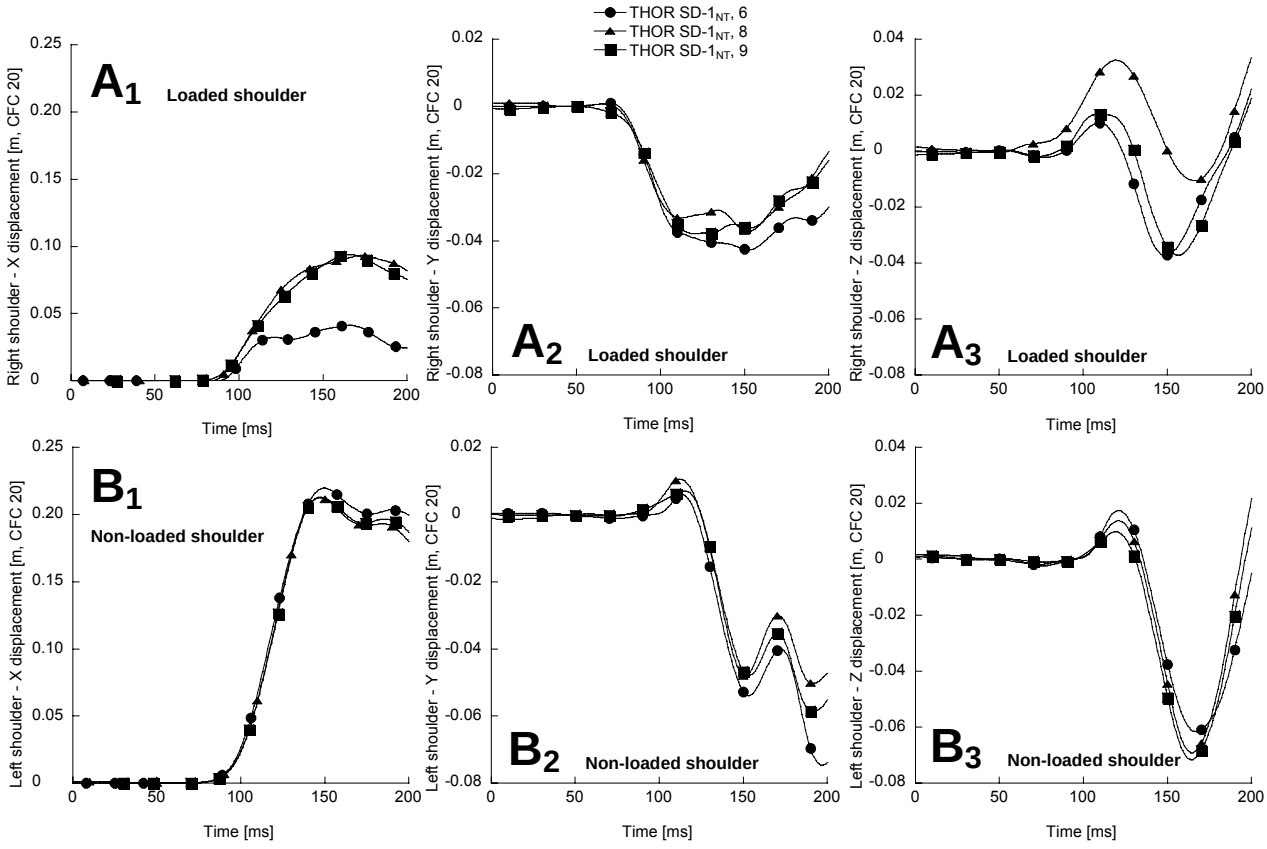

Fig. 8 – Shoulder rel. to T1 displacements of the loaded (A) and non-loaded (B) shoulders in the anterior-posterior, (A_1 and B_1), lateral-medial, (A_2 and B_2) and superior-inferior (A_3 and B_3) directions.

LIMITATIONS AND SOURCES OF ERROR: In the experiments some factors could not be fully controlled. Possible sources of errors are listed and discussed below.

- The film targets on the dummies are in few cases not positioned in exactly the same position as on the PMHSs. However, the positions of the film targets on the dummies were chosen to be as close as possible to those of the PMHSs. The influence of the difference in position on the kinematics was judged to be minor in relation to inter-PMHSs differences.
- Prior to each test, the belt was carefully positioned on the shoulder with guidance of photos of previous tests. The method may have caused differences which could have had minor influences on the body kinematics. In the analysis these differences were judged to be small in relation to the differences in individual PMHSs responses because the belt consistently slipped relative the clavicle structure in all tests.
- Errors may be introduced in the calibration of the cameras and camera positions prior to the three dimensional film analysis. To test the influence of such an error, a random error of ±5 mm was introduced to the location of the film calibration targets used in the film analyses. The head marker of PMHS 1 was then estimated with and without introduced error. The maximum head displacement deviation was at the most ±3 mm between these two analyses.
- There may also be film target tracking errors in the kinematics analyses. The head marker of PMHS 1 in one test was tracked four times. The deviation of maximum head displacement was at most ±2 mm for the four individual trackings.

CONCLUSIONS

Four main conclusions are drawn from this study on shoulder kinematics in far-side, near-side and full-frontal collisions of the Hybrid III, THOR NT and THOR SD-1_{NT} compared with PMHS data.

- The anterior shoulder range-of-motion of the THOR SD-1_{NT} dummy is about 12 cm larger, in relation to T1, than that of the PMHS data. This is when the dummy resembles a person in driving posture. In comparison with PMHS data, the dummy also has about 4 cm larger superior shoulder range-of-motion in relation to T1. However, the range-of-motion is just one of the shoulder properties. The resemblance to the human shoulder geometry, especially the clavicle and coracoid process, may also be important for the loaded shoulder and, consequently, for the overall performance.
- The anterior shoulder range-of-motion of the THOR NT (approximately 7 cm in this study) may be fairly human-like in relation to T1 for a driver with hands held on the steering wheel.
- The PMHSs and the THOR SD-1_{NT} dummy did not slip out of the shoulder belt as easily as the THOR NT dummy in the 45° far-side impacts in this study.
- In the 30° near-side impact, the THOR SD-1_{NT} dummy can mimic the superior shoulder motion of the loaded PMHSs' shoulders in relation to T1. However, this was not so for the Hybrid III and the THOR NT. The head of the THOR SD-1_{NT} dummy moved more laterally towards the simulated car door than the head of the THOR NT.

ACKNOWLEDGMENTS

This project was supported by the Swedish Vehicle Research Program (PFF) through VINNOVA.

REFERENCES

Buzeman DG. (1997) Car-to-Car and Single Car Compatibility: Individual Effects of Mass, Structure, Stiffness and Geometry, Licentiate in Engineering, Department of Injury Prevention, Chalmers University of Technology, Göteborg, Sweden, ISBN 91-7197-536-5.

Haffner M, Eppinger R, Rangarajan N, Shams T, Artis M, Beach D. (2001) Foundations and Elements of the NHTSA Thor ALPHA ATD Design, Proc. *17th International Technical Conference on the Enhanced Safety of Vehicles*, Paper no. 2001-06-0107.

Hontschik H and Rüter G. (1980) Investigations into the Efficacy of Three-Point Seat-Belts in Oblique Impact Experiments, Proc. *International IRCOBI Conference on the Biomechanics of Impacts*, pp. 128–138.

Hoofman M, van Ratingen M, Wismans J. (1998) Evaluation of the Dynamic and Kinematic Performance of the THOR Dummy: Neck Performance, Proc. *International IRCOBI Conference on the Biomechanics of Impact*, pp. 497–511.

Kallieris D, Rizzetti A, Mattern R. (1995) The Biofidelity of Hybrid III Dummies, Proc. *International IRCOBI Conference on the Biomechanics of Impact,* pp. 135–154.

Kent R, Murakami D, Kobayashi S. (2005) Frontal Thoracic Response to Dynamic Loading: The Role of Superficial Tissues, Viscera, and the Rib Cage, Proc. *International IRCOBI Conference on the Biomechanics of Impact*, pp. 355–365.

Kent R, Lessley D, Sherwood C. (2004) Thoracic Response to Dynamic, Non-Impact Loading from a Hub, Distributed Belt, Diagonal Belt, and Double Diagonal Belts, *Stapp Car Crash Journal*, Vol. 48, No. 1, pp. 495–519.

Kent R, Lessley D, Shaw G, Crandall J. (2003) The Utility of Hybrid III and THOR Chest Deflection for Discriminating between Standard and Force-Limiting Belt Systems, *Stapp Car Crash Journal*, Vol. 47, No. 1, pp. 267–297.

Kerrigan J, Kam C, Drinkwater C, Murphy D, Bose D, Ivarsson J, Crandall J. (2005) Kinematic Comparison of the Polar-II and PMHS in Pedestrian Impact Tests with a Sport-Utility Vehicle, Proc. *International IRCOBI Conference on the Biomechanics of Impacts*, pp. 159–174.

Lindquist M, Hall A, Björnstig U. (2006) Kinematics of Belted Fatalities in Frontal Collisions: A New Approach in Deep Studies of Injury Mechanisms, *The Journal of Trauma, Injury, Infection and Critical Care*, Vol. 61, No. 6, pp. 1506–1516.

Lindquist M, Hall A, Björnstig U. (2004) Car Structural Characteristics of Fatal Frontal Crashes in Sweden, *International Journal of Crashworthiness*, Vol. 9, No. 6, pp. 587–597.

Mertz HJ. (1984) A Procedure for Normalizing Impact Response Data, Proc. *SAE Government Industry Meeting and Exposition*, Paper no. 840884, pp. 1159–1166.

Onda K, Matsuoka F, Ono K, Kubota M, Peter M, Youmei Z. (2006) Differences in the Dynamic Responses of the Thor-NT and Thor-FT Dummies, Proc. *SAE World Congress*, Paper no. 2006-01-0676, pp. 149–174.

Shaw G, Lessley D, Kent R, Crandall J. (2005) Dummy Torso Response to Anterior Quasi-Static Loading, Proc. *19th International Technical Conference on the Enhanced Safety of Vehicles*, Paper no. 05-0371.

Shaw G, Crandall J, Butcher J. (2000) Biofidelity Evaluation of the THOR Advanced Frontal Crash Test Dummy, Proc. *International IRCOBI Conference on The Biomechanics of Impact*, pp. 11–29.

Thunnissen J, Wismans J, Ewings CL, Thomas DJ. (1995) Human Volunteer Head-Neck Response in Frontal Flexion: A New Analysis, Proc. *39th Stapp Car Crash Conference*, pp. 439–460.

Törnvall FV (2008) *A New Shoulder for the THOR Dummy Intended for Oblique Collisions*, ISBN 978-91-7385-098-8, Doctor of Philosophy Thesis, Vehicle Safety, Department of Applied Mechanics, Chalmers University of Technology, Göteborg, Sweden.

Törnvall FV, Holmqvist K, Davidsson J, Svensson MY, Håland Y, Öhrn H. (2007) A New THOR Shoulder Design: A Comparison with Volunteers, the Hybrid III and THOR NT, *Traffic Injury Prevention*, Vol. 8, No. 2, pp. 205–215.

Törnvall FV, Svensson MY, Davidsson J, Flogård A, Kallieris D, Håland Y. (2005a) Frontal Impact Dummy Kinematics in Oblique Frontal Collisions: Evaluation against Post Mortem Human Subject Test Data, *Traffic Injury Prevention*, Vol. 6, No. 4, pp. 340–350.

Törnvall FV, Holmqvist K, Martinsson J, Davidsson J. (2005b) Comparison of Shoulder Range-of-Motion and Stiffness between Volunteers, Hybrid III and THOR Alpha in Static Frontal Impact Loading, *International Journal of Crashworthiness*, Vol. 10, No. 2, pp. 151–160.

UN(1958a) Agreement – Concerning the Adoption of Uniform Conditions of Approval and Reciprocal Recognition of Approval for Motor Vehicle Equipment and Parts, E/ECE324, E/ECE/TRANS/505, Regulation no. 14, Rev.1/Add.13, Rev.2/Corr.1, 3 March 1994, Geneva, Switzerland.

UN (1958b) Agreement – Concerning the Adoption of Uniform Technical Prescriptions for Wheeled Vehicles, Equipment and Parts Which Can Be Fitted and/or Be Used on Wheeled Vehicles and the Conditions for Reciprocal Recognition of Approvals Granted on the Basis of These

Prescriptions, E/ECE324, E/ECE/TRANS/505, Regulation no. 16, Rev.1/Add.15/Rev.4, 11 August 2000, Geneva, Switzerland.
Vezin J-P, Bruyere-Garnier K, Bermond F, Verriest JP. (2002) Comparison of Hybrid III, Thor-α and PMHS Response in Frontal Sled Tests, *Stapp Car Crash Conference*, Vol. 46, No. 1, pp. 1–26.
Vezin J-P, Bruyère K, Bermond F. (2001) Comparison of Head and Thorax Cadaver and Hybrid III Responses to a Frontal Sled Deceleration for the Validation of a Car Occupant Mathematical Model, Proc. *17th International Technical Conference on the Enhanced Safety of Vehicles,* Paper No. 2001-06-0035.
White RP, Rangarajan N, Haffner M. (1996) Development of the THOR Advanced Frontal Crash Test Dummy, Proc. *34th Annual Symposium–SAE Assosiation*, pp. 122–135.
Wismans J, Spenny CH. (1984) Head-Neck Response in Frontal Flexion, Proc. *28th Stapp Car Crash Conference*, pp. 313–331.
Yoganandan N, Skrade D, Pintar FA, Reinartz J, Sances A. (1991) Thoracic Deformation Contours in a Frontal Impact, Proc. *35th Stapp Car Crash Conference*, pp. 47–63.

APPENDIX A (X-Y TRAJECTORIES)

PMHS 1
PMHS 2
PMHS 3, Test 1
PMHS 3, Test 2
Hybrid III
THOR NT
THOR SD-1$_{NT}$, Test 1
THOR SD-1$_{NT}$, Test 2
THOR SD-1$_{NT}$, Test 3

The THOR NT slipped out of the shoulder belt in the 45˚ far-side test set-up. Then the belt was caught by the accelerometer on the right arm at 140 ms. Therefore, all THOR NT data after 140 ms in the 45˚ far-side test has been masked.

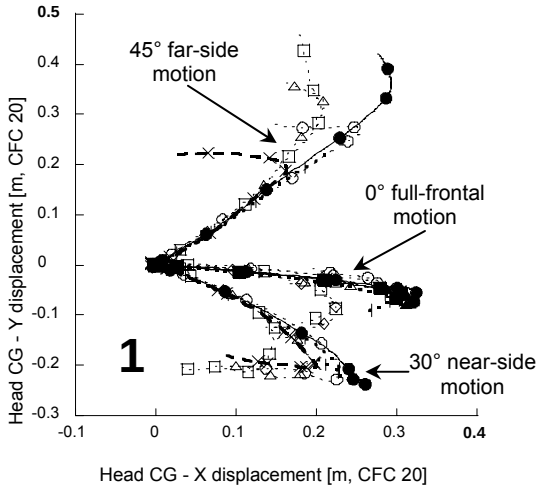

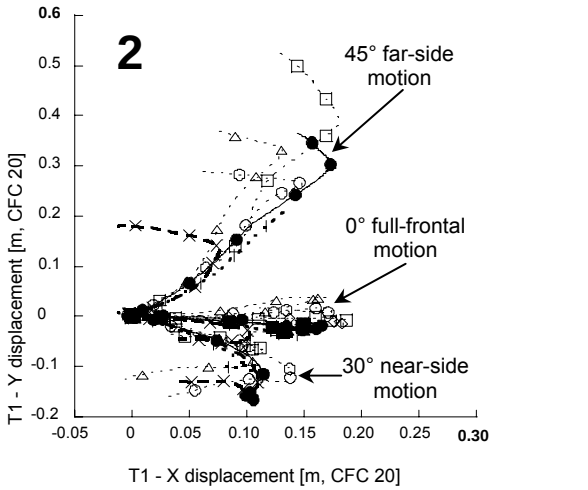

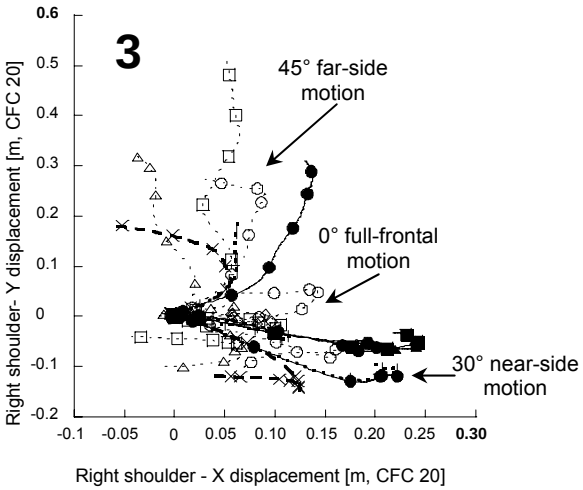

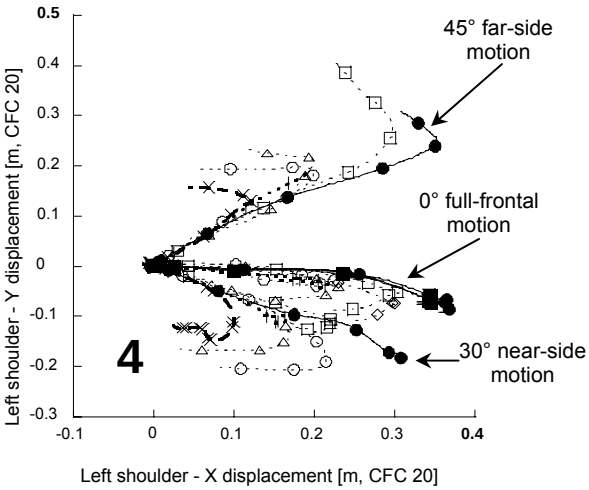

APPENDIX B (DISPLACEMENTS IN RELATION TO T1)

45˚ far-side tests

The THOR NT slipped out of the shoulder belt in the 45˚ far-side test set-up. Then the belt was caught by the accelerometer on the right arm at 140 ms. Therefore, all THOR NT data after 140 ms in the 45˚ far-side test has been deleted.

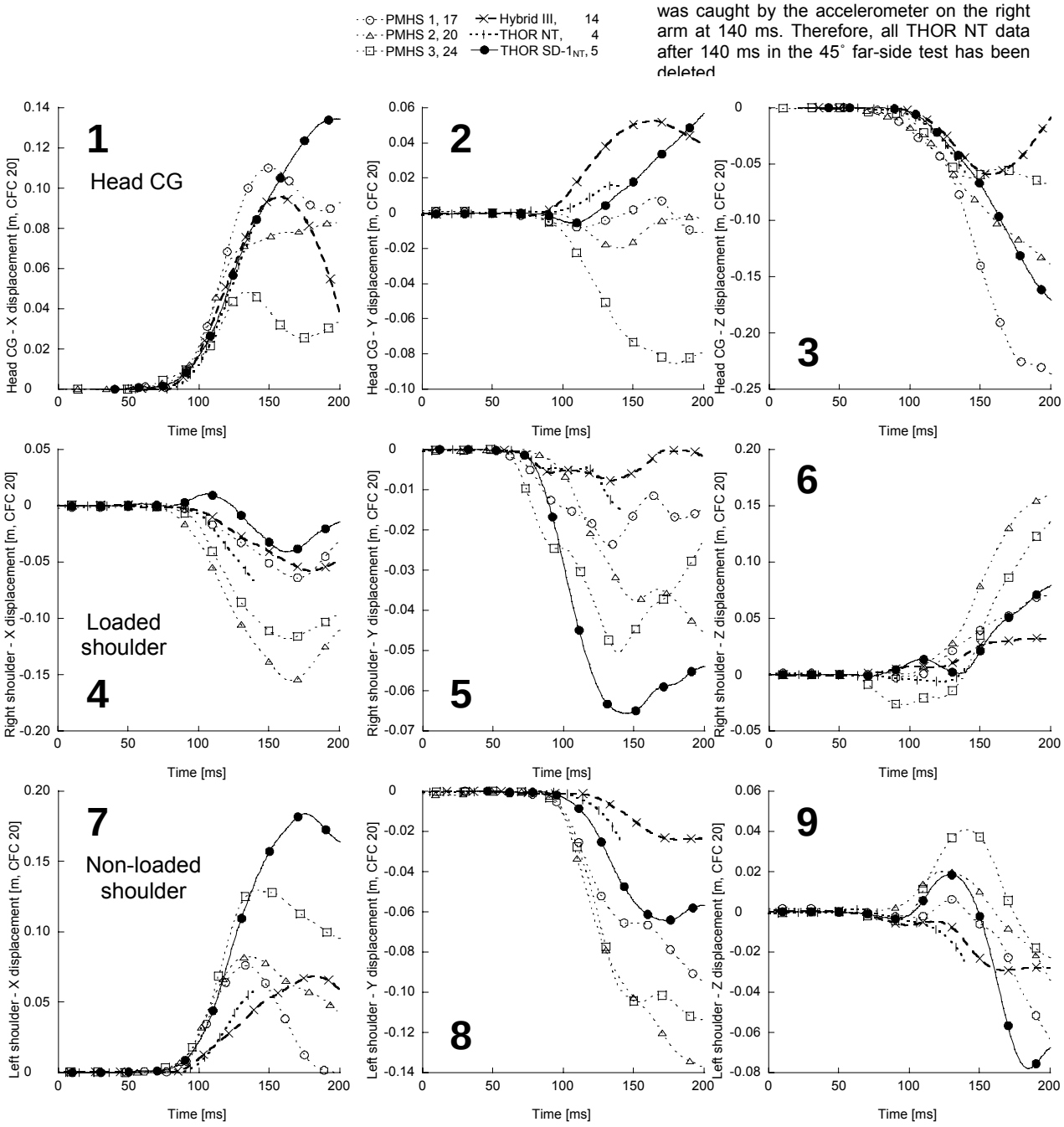

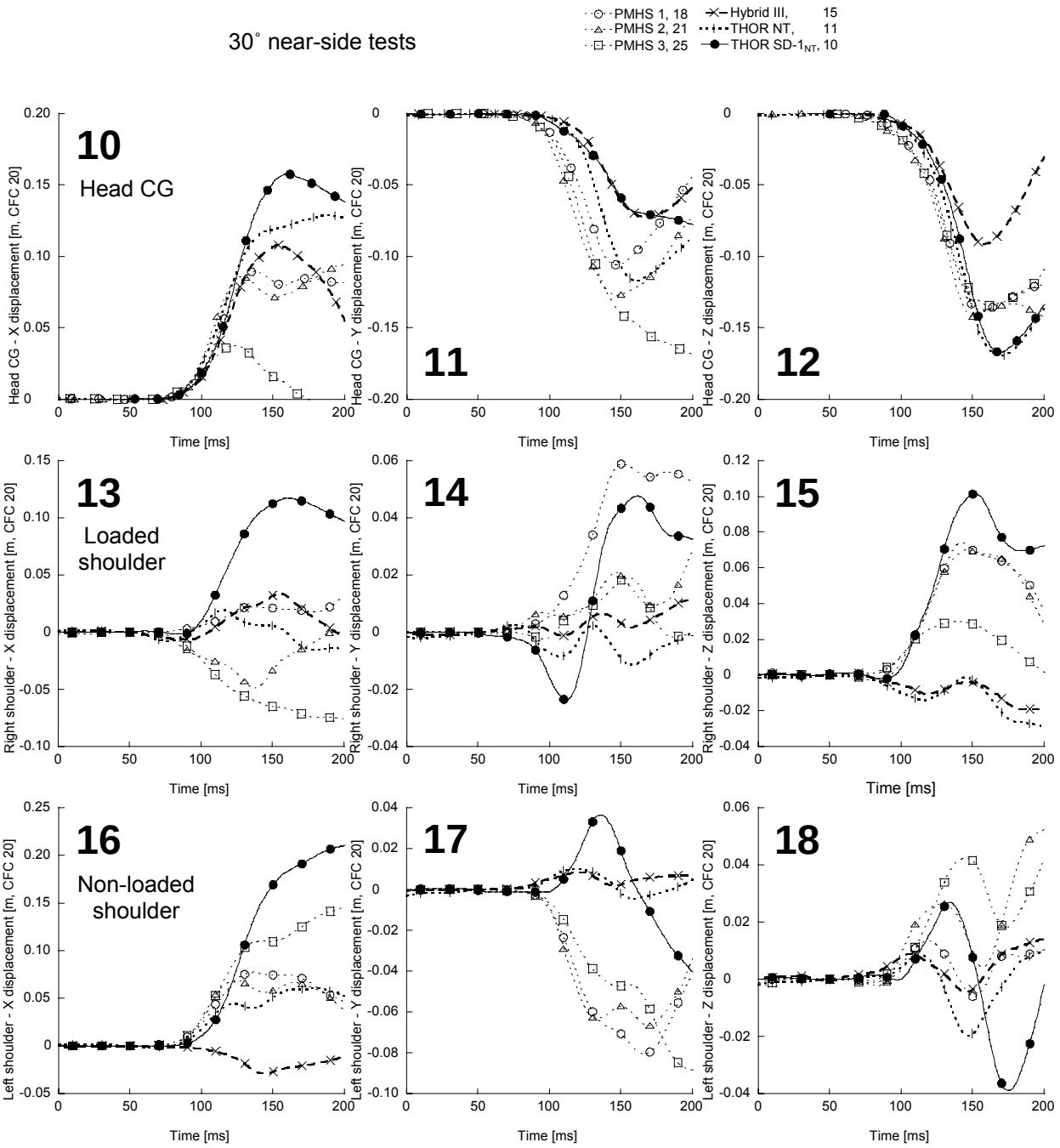
30˚ near-side tests
PMHS 1, 18
PMHS 2, 21
PMHS 3, 25
Hybrid III, 15
THOR NT, 11
THOR SD-1NT, 10
10
Head CG
Head CG - X displacement [m, CFC 20]
11
Head CG - Y displacement [m, CFC 20]
12
Head CG - Z displacement [m, CFC 20]
13
Loaded shoulder
Right shoulder - X displacement [m, CFC 20]
14
Right shoulder - Y displacement [m, CFC 20]
15
Right shoulder - Z displacement [m, CFC 20]
16
Non-loaded shoulder
Left shoulder - X displacement [m, CFC 20]
17
Left shoulder - Y displacement [m, CFC 20]
18
Left shoulder - Z displacement [m, CFC 20]
Time [ms]

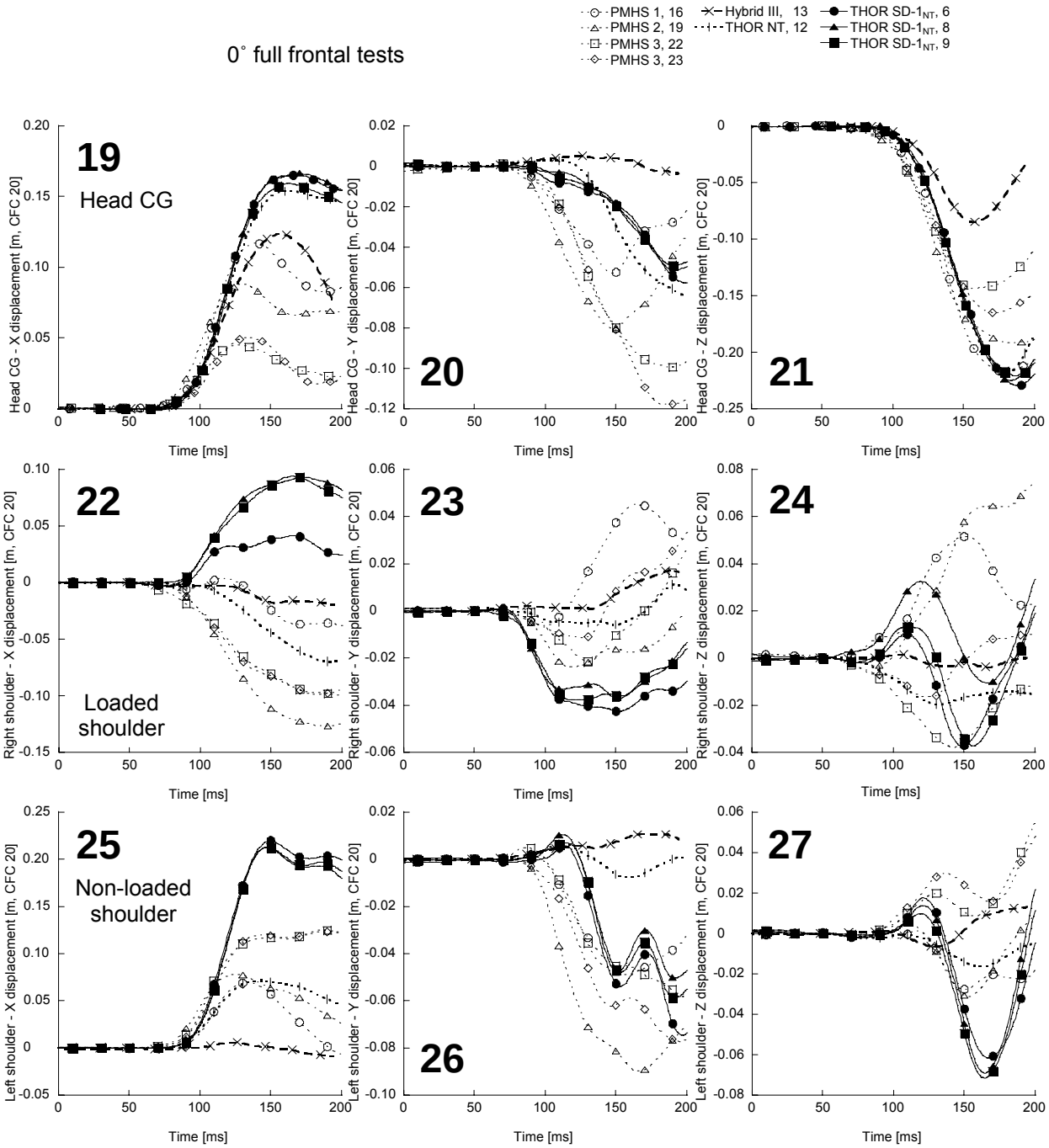
0˚ full frontal tests
PMHS 1, 16
PMHS 2, 19
PMHS 3, 22
PMHS 3, 23
Hybrid III, 13
THOR NT, 12
THOR SD-1NT, 6
THOR SD-1NT, 8
THOR SD-1NT, 9
19
Head CG
Head CG - X displacement [m, CFC 20]
20
Head CG - Y displacement [m, CFC 20]
21
Head CG - Z displacement [m, CFC 20]
22
Loaded shoulder
Right shoulder - X displacement [m, CFC 20]
23
Right shoulder - Y displacement [m, CFC 20]
24
Right shoulder - Z displacement [m, CFC 20]
25
Non-loaded shoulder
Left shoulder - X displacement [m, CFC 20]
26
Left shoulder - Y displacement [m, CFC 20]
27
Left shoulder - Z displacement [m, CFC 20]
Time [ms]